



UCRL-ID-108158

**PCMDI Report No. 9**

**A MODELING PERSPECTIVE  
ON CLOUD RADIATIVE FORCING**

by

**Gerald L. Potter<sup>1</sup>, Julia M. Slingo<sup>2</sup>, Jean-Jacques Morcrette<sup>3</sup> and Lisa Corsetti**

**<sup>1</sup> Program for Climate Model Diagnosis and Intercomparison  
Lawrence Livermore National Laboratory, Livermore, CA, USA**

**<sup>2</sup> Department of Meteorology, University of Reading, Reading, Berkshire, UK**

**<sup>3</sup> European Centre for Medium-Range Weather Forecasts,  
Reading, Berkshire, UK**

**February 1993**

**PROGRAM FOR CLIMATE MODEL DIAGNOSIS AND INTERCOMPARISON  
UNIVERSITY OF CALIFORNIA, LAWRENCE LIVERMORE NATIONAL LABORATORY  
LIVERMORE, CA 94550**

## DISCLAIMER

This document was prepared as an account of work sponsored by an agency of the United States Government. Neither the United States Government nor the University of California nor any of their employees, makes any warranty, express or implied, or assumes any legal liability or responsibility for the accuracy, completeness, or usefulness of any information, apparatus, product, or process disclosed, or represents that its use would not infringe privately owned rights. Reference herein to any specific commercial products, process, or service by trade name, trademark, manufacturer, or otherwise, does not necessarily constitute or imply its endorsement, recommendation, or favoring by the United States Government or the University of California. The views and opinions of authors expressed herein do not necessarily state or reflect those of the United States Government or the University of California, and shall not be used for advertising or product endorsement purposes.

This is an informal report intended primarily for internal or limited external distribution. The opinions and conclusions stated are those of the author and may or may not be those of the Laboratory.

This report has been reproduced  
directly from the best available copy.

Available to DOE and DOE contractors from the  
Office of Scientific and Technical Information  
P.O. Box 62, Oak Ridge, TN 37831  
Prices available from (615) 576-8401, FTS 626-8401

Available to the public from the  
National Technical Information Service  
U.S. Department of Commerce  
5285 Port Royal Rd.,  
Springfield, VA 22161

## ABSTRACT

Radiation fields from a perpetual July integration of a T106 version of the ECM-WF operational model are used to identify the most appropriate way to diagnose cloud radiative forcing in a general circulation model, for the purposes of intercomparison between models. Differences between the Methods I and II of Cess and Potter (1987) and a variant method are addressed. Method I is shown to be the least robust of all methods, due to the potential uncertainties related to persistent cloudiness, length of the sampling period and biases in retrieved clear-sky quantities due to insufficient sampling of the diurnal cycle.

Method II is proposed as an unambiguous way to produce consistent radiative diagnostics for intercomparing model results. The impact of the three methods on the derived sensitivities and cloud feedbacks following an imposed change in sea surface temperature is discussed. The sensitivity of the results to horizontal resolution is considered by using the diagnostics from parallel integrations with T21 version of the model.

## 1. Introduction

The concept of cloud radiative forcing was first discussed in the open literature by Coakley and Baldwin (1984) and was first used by Ramanathan (1987) to identify the impact of clouds on the radiation budget at the top of the atmosphere. It may be defined as the difference between the radiative flux which actually occurs with cloudiness and that which occurs for clear skies. The change in cloud radiative forcing which accompanies a change in climate is known as cloud feedback. In a recent study by Cess et al. (1989,1990) of the response of 19 atmospheric general circulation models (GCMs) to an imposed change in sea surface temperature (used as a surrogate climate change), an almost threefold variation in the cloud feedback from weakly negative to strongly positive was obtained. This led Cess et al. to conclude that cloud-climate feedback could be a significant cause of inter-model differences in climate change projections. In subsequent analysis of the individual modeling results, it has become apparent that there are a number of different approaches used in the computation of cloud radiative forcing.

In terms of the energy lost or gained by the earth-atmosphere system, cloud forcing (CRF) can be defined as:

$$\text{CRF} = F_{\text{clear}} - F_{\text{total}} + Q_{\text{total}} - Q_{\text{clear}} \quad (1)$$

where  $F$  and  $Q$  are, respectively, the emitted infrared and net downward solar fluxes at the top of the atmosphere (TOA). The concept of cloud radiative forcing was originally introduced with satellite data because it allowed the impact of clouds on the TOA radiation budget, and therefore on the earth/atmosphere system, to be determined without requiring any knowledge of the cloud fraction or cloud height, both of which are difficult to measure. Similarly, the modeling community has adopted cloud radiative forcing because it circumvents the problems of comparing or validating cloud amount and cloud radiative properties, both of which are highly model dependent.

The primary uncertainty in the calculation of cloud radiative forcing lies in the determination of the clear sky fluxes. The original estimates of cloud radiative forcing were computed from satellite data in which the clear sky flux could only be obtained from cloud free pixels. The basic assumption was made that, over a reasonable length of time, say one month, the majority of pixels would experience clear skies at some

time and thus allow measurement of clear sky flux. While this appears to be the only practical way for estimating the clear sky flux from satellite data, it has the disadvantage that the clear and cloudy fluxes do not apply to the same atmospheric state. Additionally, it is conceivable that there may be areas of the globe where the satellite is unable to find any clear pixels and thus unable to estimate the cloud radiative forcing. Cess and Potter (1987) identified this calculation of the clear sky flux as Method I and used it in the context of a general circulation model by equivalencing the model grid to the satellite pixels. In this paper, it will be referred to as Method Ia to distinguish it from the variant of this method used by many participants in the intercomparison study of Cess et al. (1989,1990), whose models employed a fractional cloud scheme.

An alternative procedure exists for models, in which the clear sky flux is computed whatever the cloudiness. This flux is often already available from the radiation code or can be computed easily by running the code again with clear skies. This method of calculating the cloud radiative forcing was defined as Method II by Cess and Potter (1987) and gives a cloud forcing which represents the impact of the clouds on the radiative fluxes for the same atmospheric state. This is an important point as will become apparent in the later discussion.

More recently, a hybrid version, intermediate between Methods Ia and II, has been used in a number of models which employ a fractional cloud prediction scheme. Referred to in this paper as Method Ib, it weights the clear sky flux, computed as in Method II, by the clear sky fraction. Although not specifically requested in the Cess et al. (1989,1990) intercomparison study, Method Ib was used by all but one of the participants whose model includes a fractional cloud scheme.

In this paper, radiative fields at the TOA from a series of integrations of the ECMWF general circulation model, run at two different horizontal resolutions are used to study the validity of the methods for retrieving the clear sky flux, specifically in the context of model intercomparison and for the estimation of the cloud feedback in studies of climate change. The various methods of retrieving the clear sky fluxes are described in Section 2. In Section 3, the uncertainties inherent to Method Ia are reviewed. Methods II and Ib results are shown in Sections 4 and 5, respectively. Section 6 discusses how the differences in clear-sky fluxes obtained by the various methods might influence the sensitivity of the model to an imposed change in sea surface temperature (SST). The dependence of the results on the model's horizontal resolution is also considered.

## 2. Methodology - Description of Methods Ia, Ib and II

### a. *The model*

A general description of the ECMWF forecasting system is given in Hollingsworth et al. (1985). More detailed discussions of the dynamical and physical parameterization aspects of the model are found in Simmons et al. (1988) and Tiedtke et al. (1988), respectively.

In the ECMWF model, the prognostic variables are represented in the horizontal by truncated series of spherical harmonics. The model uses a triangular truncation; T106 horizontal resolution therefore refers to the representation retaining the first 106 spectral coefficients. Physical tendencies are calculated by the physical processes parameterizations on a Gaussian collocation grid where the mesh size is (1.125) at T106 and (5.625) at T21. All results presented hereafter were obtained with the ECMWF model running at PCMDI (cycle 33 of the libraries, operational in July 1989). In particular, the model includes the new mass-flux scheme for parameterizing convective processes (Tiedtke, 1989) and the new radiation scheme (Morcrette, 1990). Cloud fields are diagnosed with the original cloud scheme of Slingo (1987). The model includes the diurnal cycle of insolation. Full radiation computations are performed every 3 hours and the radiation fields are updated at every time step ( $\Delta t = 900\text{s}$  at T106,  $\Delta t = 2700\text{s}$  at T21) taking into account the correct solar zenith angle in the shortwave and the correct temperature profile in the longwave computations.

The model was integrated for 90 days for perpetual July conditions using either the climatological SSTs of Alexander and Mobley (1976) in the control case, or 2K SST perturbations to that climatology in the perturbed cases (SST-2K, SST+2K). In all the integrations, instantaneous total and clear-sky radiation fields were saved every 3 hours. Most results are means over the last 30 days of the integrations and therefore include the average of 240 instantaneous fields.

b. *Clear sky flux retrievals*

In Method Ia (I) as described by Cess and Potter (1987) and used by Harshvardhan et al. (1989), the time averaged clear sky flux for any model grid point is obtained from:

$$F_{cs} = \frac{\sum_{i=1}^N F_i \delta_i}{\sum_{i=1}^N \delta_i} \quad (2)$$

where  $N$  is the total number of samples (here the total number of radiation time-steps) and  $\delta_i$  is 1 if the grid is totally clear and 0 otherwise.  $F_i$  is the total flux so that only the fluxes for clear sky conditions are summed in this case. Cess and Potter (1987) used the diurnal average solar insolation to calculate absorbed clear sky solar flux while this paper calculates the clear sky flux in a way similar to Harshvardhan et al. (1989). Both averaging methods give areas with missing clear sky "observations" wherever there is always some fractional cloudiness (not necessarily overcast). If a model includes a diurnal cycle, then Method Ia is also likely to lead to a different sampling for longwave and shortwave fluxes.

With Method II, the clear sky flux is computed from the temperature and humidity profiles and is therefore available at every point and at every time. Thus the time averaged clear sky flux in a grid box is simply given by:

$$F_{cs} = \frac{1}{N} \sum_{i=1}^N F_i^{\text{clear}} \quad (3)$$

where  $F_i^{\text{clear}}$  is the clear sky flux computed by the model. In principle, this method can always be applied in model calculations of the cloud radiative forcing, since the clear sky flux is always defined whatever the conditions. In practice, depending on the actual details of the radiation code, this method may require running the radiation code twice; once for computing the diagnostic clear sky fluxes and once for calculating

the total fluxes and radiative heating rates required by the thermodynamic equation of the model.

Method Ib is intermediate between Methods Ia and II. In the context of a model simulation, the time averaged clear sky flux is computed using:

$$F_{cs} = \frac{\sum_{i=1}^N F_i^{\text{clear}} (1 - c_i)}{\sum_{i=1}^N (1 - c_i)} \quad (4)$$

where  $c_i$  is the total cloudiness as seen from the top of the atmosphere over the grid-box at time-step  $i$ , and  $F_i^{\text{clear}}$  is the clear sky flux computed by the model. This method has often been adopted as a variant of Method Ia by modelers whose cloud scheme allows for partial cloudiness. Again, it assumes knowledge of the clear sky flux at every grid point for every time sample, as in Method II. However, unlike Method II, it will be prone to sampling problems because the cloud radiative forcing will not be defined for overcast conditions. Thus, in the case of an “on/off” cloud scheme (cloud cover is either 0 or 1), Method Ib is equivalent to Method Ia.

None of these three methods is consistent with the elaborate data processing carried out on ERBE measurements. For the purpose of validating the results from GCMs against ERBE data, another method for calculating the cloud forcing is required and is described in Cess et al. (1992). This is a distinct problem from the question of model intercomparison which this paper is intended to address.

### 3. Results: Method Ia

As already described, the cloud radiative forcing calculated using Method Ia is dependent on the number of samples for which the sky is clear during the time period in question. Figure 1 shows the percentage incidence of clear skies for the mean of days 61 to 90 from the T106 model. The corresponding cloud amounts are shown in Figure 2. The grey areas in Figure 1 represent missing data, i. e. those grid points for which there were no cloud-free days. These occur primarily over the convectively

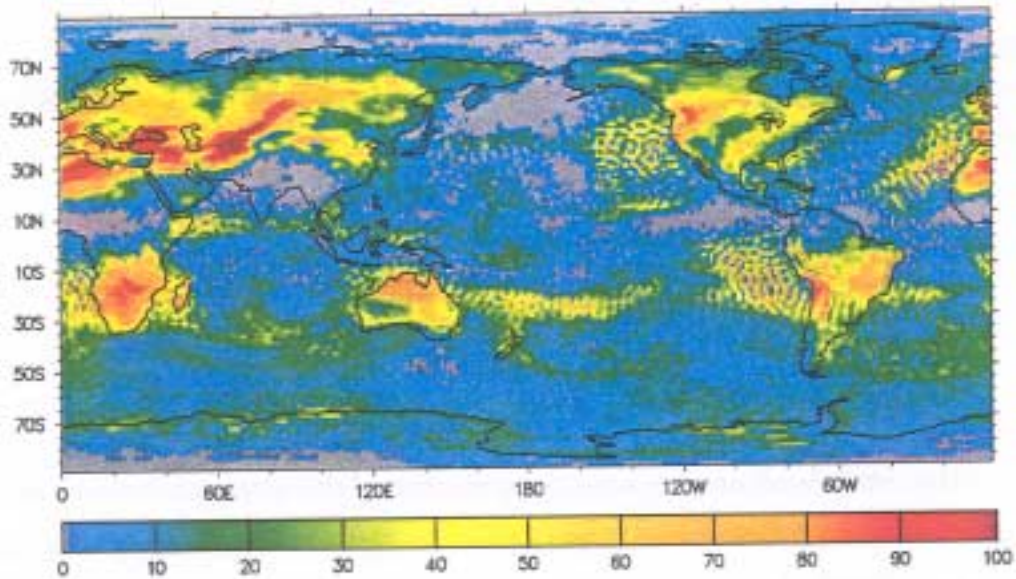


Fig.1. The percentage incidence of clear-sky observations during the last 30 days of a T106 90-day perpetual July integration.

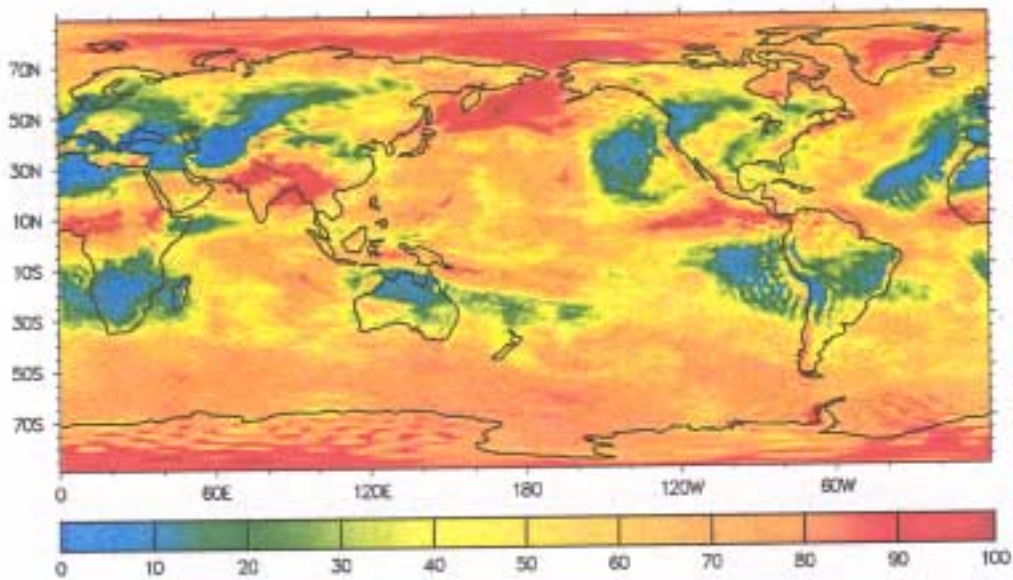


Fig. 2. The mean total cloudiness (%) during the last 30 days of a T106 90-day perpetual July integration.

active areas of the tropics and over the region of persistent stratus associated with the cold waters of the North Pacific. The area of missing data over the Himalayas is primarily due to the model's tendency for the monsoon flow over India to track northwards, releasing its precipitation over this region, rather than over India itself.

It is clear from Figures 1 and 2 that the main areas of missing data are coincident with the areas of maximum cloudiness, precisely where the cloud radiative forcing will be large. Similarly, Figure 1 also shows that the percentage incidence of clear skies is low over most regions of the globe with good correlation between large amounts of cloud and low percentages of incidence of clear skies. Where the cloud radiative forcing is likely to be large, Method Ia will therefore rely on a small number of samples. Thus, both in terms of missing data and of sample size, the cloud radiative forcing is likely to be poorly represented by Method Ia in those regions where it is important.

The areas of missing data in this 30-day mean from the ECMWF model run at T106 horizontal resolution are quite extensive and probably arise from the model's tendency to produce a persistent location for the ITCZ, which is more marked at higher resolution. Thus, it could be argued that an intercomparison of the cloud radiative forcing from different models or from different resolutions might not be particularly informative because the areas of missing data will not be the same. The question of sample size also has to be considered. For model intercomparison, it is possible that the sampling may be dependent on the type of cloud scheme used in a model. An "on/off" cloud scheme may show a greater incidence of clear skies than a fractional cloud scheme.

It is clear from the description of Method Ia that it is only valid in a time mean sense and cannot be used to identify the instantaneous cloud radiative forcing. Thus it will be dependent on the length of the time mean. The longer the averaging period the more likely it is that a region will experience clear skies so that the areas of missing data should become smaller. Figure 3 shows the number of missing data for each latitude row of the T106 model for 10, 30 and 90 day averaging periods. There are substantial differences between the distributions based on 10 and 30-day averaging periods at most latitudes. With an increase in the averaging period to 90 days, the decrease in the number of missing data is less marked, reflecting the persistent nature of the ITCZ, the clouds over the Himalayan plateau and the stratus over the cold waters of the North Pacific. The results suggest that a 30-day average is the minimum

necessary to remove the effects of the transient features such as the southern hemisphere depression belt.

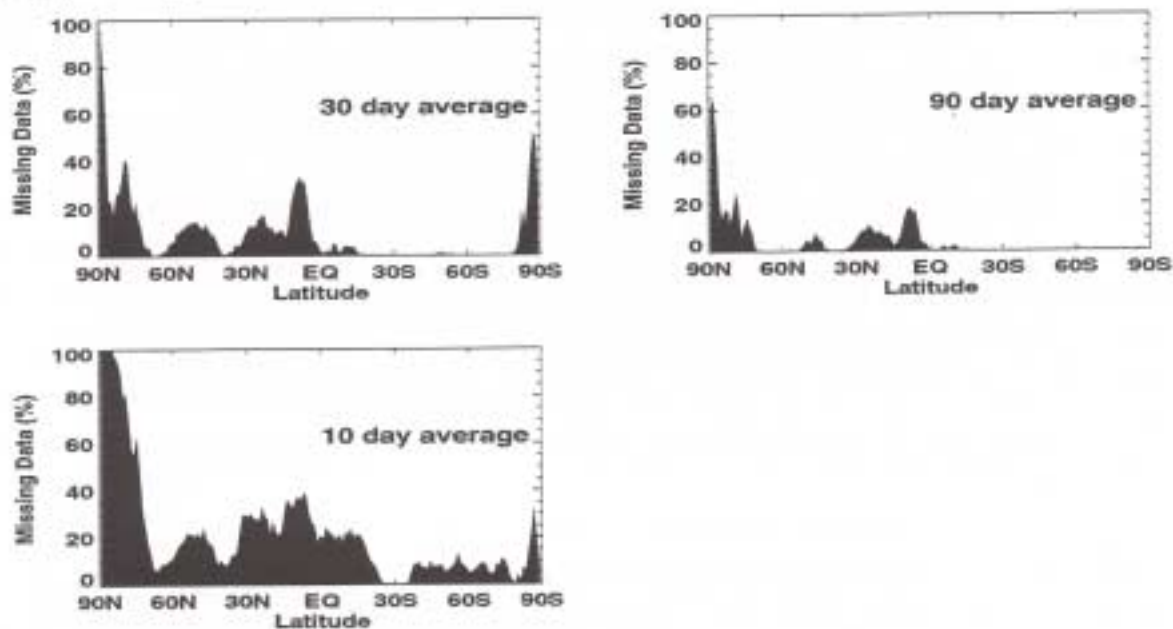


Fig. 3. The number of missing data for each latitude row of the T106 model for 10, 30 and 90 day averaging periods.

The diurnal variation in convective activity over the tropical continents has been well documented (e.g. Minnis and Harrison, 1984; Harrison et al., 1988). Typically, over land, it shows a peak in cloudiness in the afternoon with a minimum in the early hours of the morning. This suggests that a diurnal bias in the sampling, particularly for the shortwave cloud forcing, might be a problem for Method Ia. Over the Amazon Basin, for example, the model shows a tendency for more missing data to occur at 18 GMT, compared with other times of the day, associated with the onset of daytime convection. Thus, in this region, the clear sky flux and hence the shortwave cloud forcing may be biased towards early morning or late afternoon values and the peak forcing near noon may not be sampled properly. The longwave cloud forcing is likely to display a diurnal bias also, but in a much less marked sense, through the diurnal variation in the land surface temperature.

The shortwave cloud forcing (SCF) computed using Method Ia for the T106 model is shown in Figure 4. It is derived from monthly averaged fluxes:

$$SCF = Q_{total} - Q_{clear} \quad (5)$$

where  $Q_{\text{total}}$  is the total downward shortwave flux, averaged over the 240 samples, and is the clear sky downward shortwave flux, averaged over the clear sky samples only. The extreme negative and positive values in Figure 4 are artifacts of the diurnal

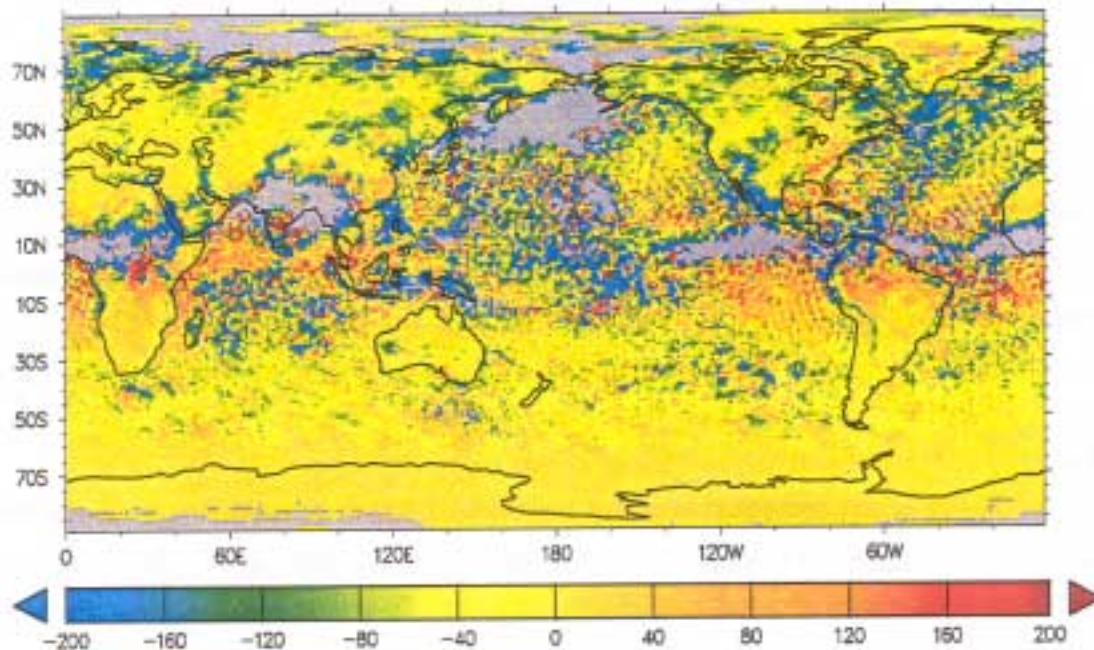


Fig. 4. The shortwave cloud forcing computed using Method 1a from time averaged fluxes, for the last 30 days of a T106 90-day perpetual July integration.

sampling problem already discussed. While the global mean shortwave forcing  $-44.0 \text{ Wm}^{-2}$  is reasonable, the details of the two dimensional distribution are clearly not. The excessive negative values occur because the clear sky flux is only sampled near local noon, with the consequence that the time averaged clear sky flux is an overestimation of the true daily averaged clear sky flux. Similarly the extreme positive values of the forcing are due to the clear sky flux only being sampled either in the early morning or late afternoon, thus giving a value which is unrealistically small and hence implying a large positive shortwave forcing. It is interesting to note that these extreme values of shortwave cloud forcing are located close to areas of missing data and are coincident with the areas of low percentage incidence of clear skies (generally less than 10%) shown in Figure 1. The Method 1a used by Cess and Potter (1987) produces similar, but less extreme positive and negative fluxes (not shown).

The combination of the areas of missing data and the extreme values in regions of poor sampling would seem to make Method 1a impossible to use for the shortwave

cloud forcing, particularly in a model which incorporates a diurnal cycle. However, some of the diurnal sampling problems can be overcome by resorting to the use of clear and cloudy sky albedos rather than fluxes. In this case the shortwave cloud forcing becomes:

$$SCF = (\alpha_{\text{clear}} - \alpha_{\text{total}}) Q_{\text{in}} \quad (6)$$

where  $\alpha$  is the planetary albedo and  $Q_{\text{in}}$  is the time averaged incoming shortwave flux at the top of the atmosphere. As for the fluxes,  $\alpha_{\text{total}}$  is evaluated over the 240 samples whereas  $\alpha_{\text{clear}}$  is the mean over the clear sky samples only. The diurnal variation in the solar radiation is effectively removed by the use of albedos and the time averaged insolation. The shortwave cloud forcing computed using the albedos rather than the fluxes is shown in Figure 5. The extreme values have been removed and the main drawbacks of Method Ia are now the areas of missing data.

The problem of diurnal bias has not been completely resolved by the use of equation (6) because the surface albedo over the oceans is a function of solar zenith angle. Starting from a low generic surface albedo ( $\alpha_s = 0.07$ ), the radiation scheme produces a much higher value for the clear sky surface albedo over the ocean at low solar elevation ( $\alpha_s = 0.169$  for  $\theta = 85$ ) than it does for high solar elevations ( $\alpha_s = 0.086$  for  $\theta = 5$ ). As well as the surface albedo, the Rayleigh scattering also has a zenith angle dependence which will affect the clear sky albedo.

It is evident from the above discussion that the cloud radiative forcing determined from Method Ia will depend on whether a model includes a diurnal cycle or not. Similarly, it may also depend on the model's convective and cloud parameterization schemes and the response of those schemes to the diurnal variation in surface heating. Harshvardhan et al. (1989) have noted that the cloud radiative forcing in the UCLA/GLA GCM, calculated using Method Ia, is influenced by that model's tendency to produce more cloud at night.

While the shortwave forcing is dominated by cloud amount, the longwave forcing is also dependent on cloud height, the colder the cloud's radiating temperature relative to the temperature of the underlying surface, the greater the longwave forcing. The longwave cloud forcing computed using Method Ia is shown in Figure 6. As with the shortwave cloud forcing (Figure 5), the main areas of missing data occur in similar locations, along the ITCZ, over the Himalayas and cold waters of the North Pacific.

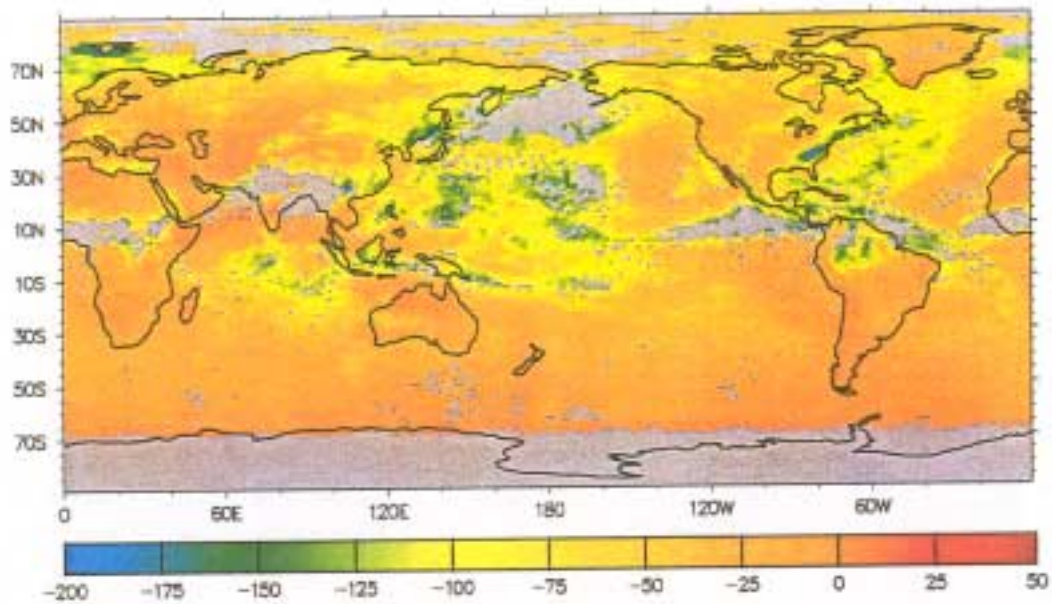


Figure 5: The shortwave cloud forcing computed using Method Ia from time averaged albedos, for the last 30 days of a T106 90-day perpetual July integration.

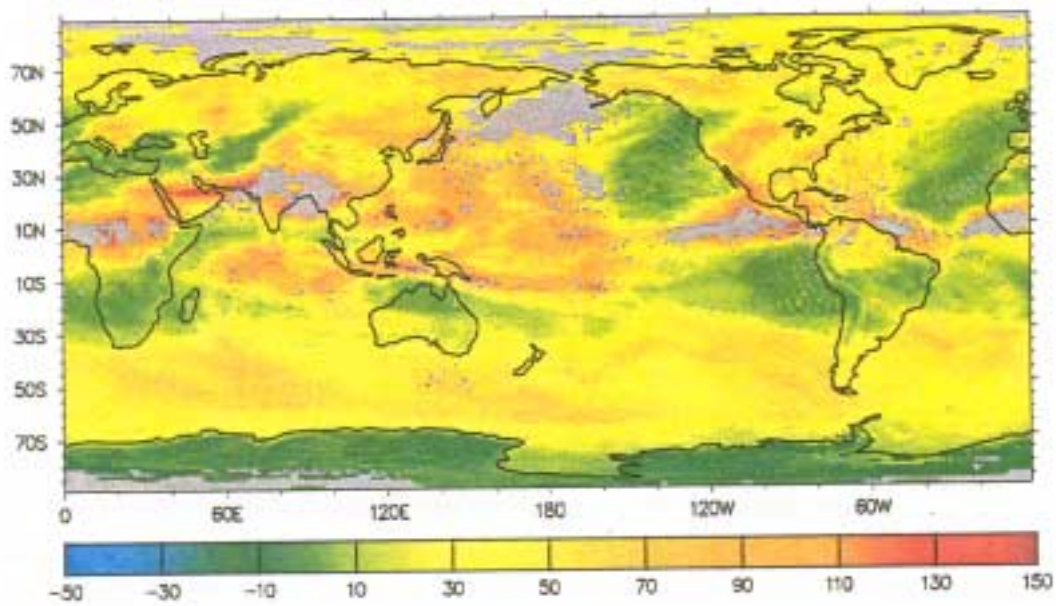


Figure 6: The longwave cloud forcing computed using Method Ia, for the last 30 days of a T106 90-day perpetual July integration.

#### 4. Results: Method II.

The shortwave cloud forcing computed using Method II is shown in Figure 7. Comparison with Figure 5 confirms the supposition that, due to the areas of missing data, Method Ia may underestimate the shortwave cloud forcing by a considerable amount.

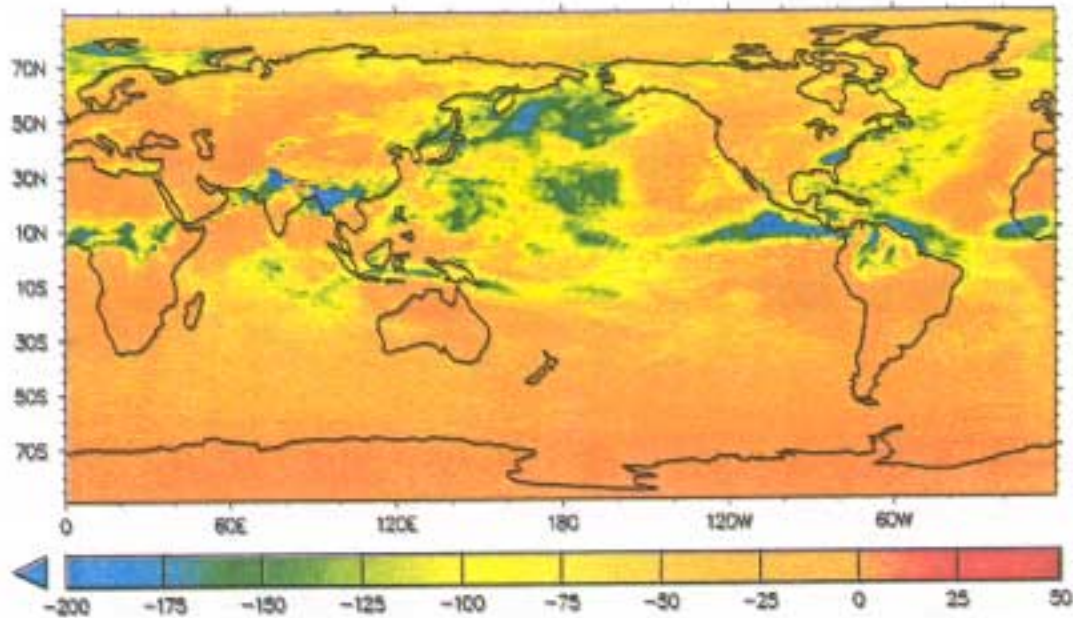


Fig.7. The shortwave cloud forcing computed using Method II, for the last 30 days of T106 90-day perpetual July integration.

Figure 8 shows the longwave cloud forcing computed using Method II. The main areas of longwave forcing are associated with the dense cirrus clouds of the convectively active regions of the tropics. The low level stratus clouds of the North Pacific, important in the shortwave forcing (Figure 7), have little impact on the longwave forcing. The main differences between the longwave cloud forcing computed by Methods Ia and II (Figures 6 and 8) are again in the areas of missing data, coincident with the regions of deep convection in the tropics. Other small differences are evident, particularly over the continents of the summer hemisphere. These are due to sampling problems in Method Ia such that the clear sky values are not representative of the same atmospheric and surface conditions used to compute the total fluxes. Over land,

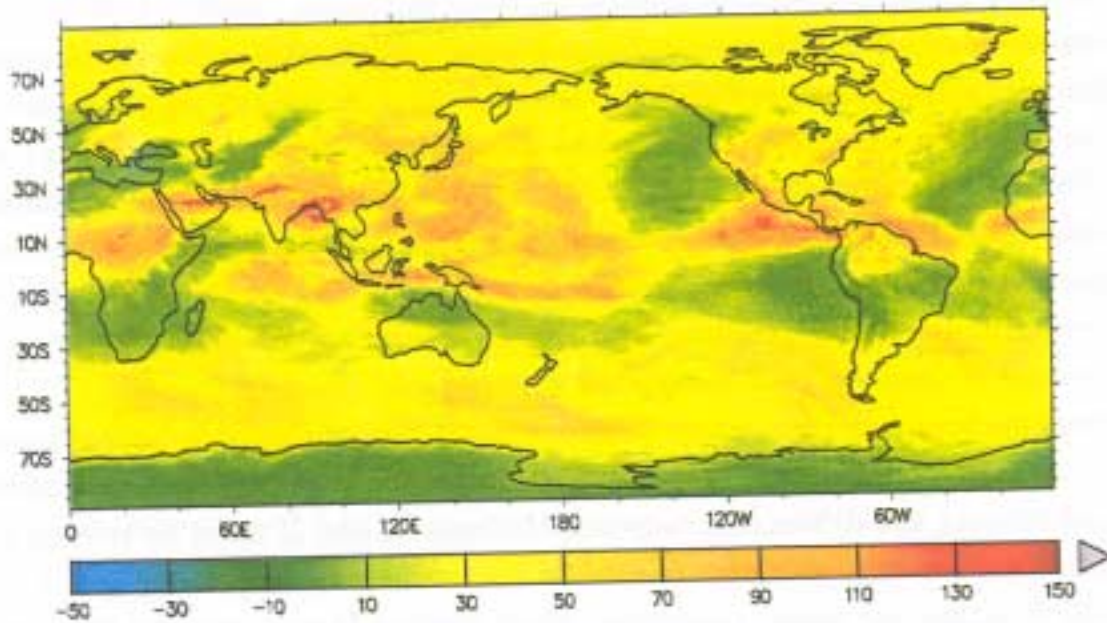


Fig. 8 The longwave cloud forcing computed using Method II, for the last 30 days of a T106 90-day perpetual July integration.

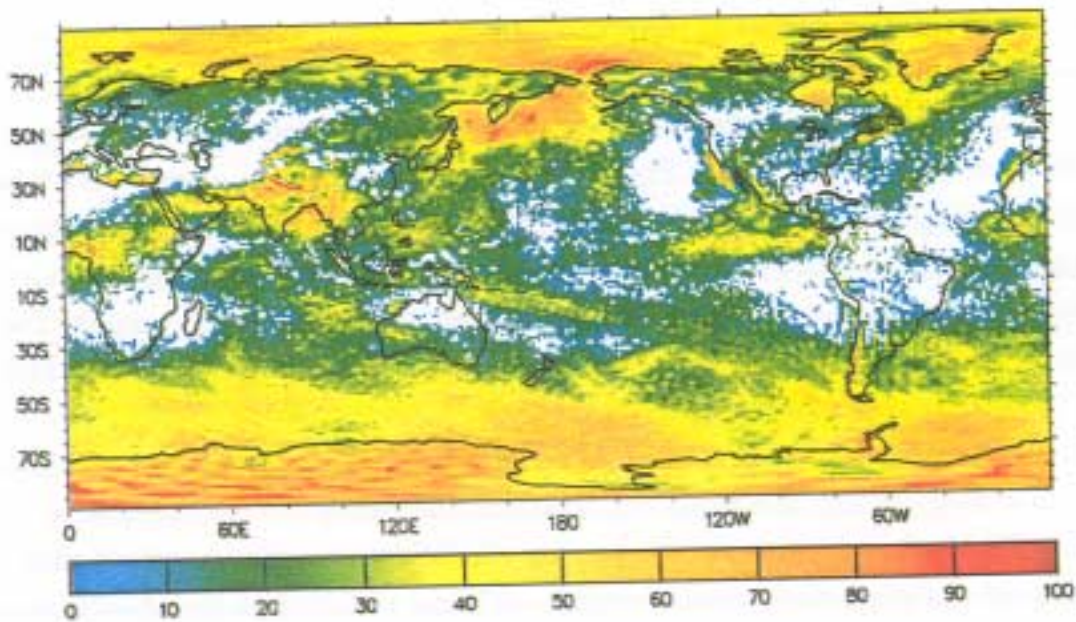


Fig. 9. The percentage incidence of overcast observations during the last 30 days of a T106 90-day perpetual July integration.

such as East Asia and the United States, the clear sky fluxes will tend to be associated with warmer surface temperatures due to greater solar heating with clear skies. It is possible that some of this tendency to overestimate the clear sky longwave flux with Method Ia will be reduced or exacerbated depending on the sampling of the diurnal cycle. For example, in the UCLA/GLA GCM, Harshvardhan et al. (1989) attribute the excessive clear sky OLR, and hence the overestimation of the longwave cloud forcing computed using Method Ia (their Method I), to the tendency for the model to produce low stratocumulus clouds over land at night, so preventing sampling of the relatively small values of clear sky OLR associated with the cold ground.

Over the southern hemisphere oceans, where there can be little diurnal variation in cloudiness and no variation in the surface temperature (as SSTs are fixed at climatological values), the differences between Methods Ia and II must be related to the tendency for clear sky conditions to contain less water vapor and thus give a higher clear sky flux than for cloudy conditions. Since Method Ia only samples the clear sky atmospheric state, then it will be biased towards drier conditions.

## **5. Results: Method Ib.**

For the ECMWF model, the characteristics of Method Ib are very similar to those of Method II and so only a limited number of results will be discussed. As described in Section 2.2, Method Ib is affected by sampling problems because the clear sky flux is not defined for overcast skies. Figure 9 shows the incidence of overcast "observations" during the 30-day period. Comparison with the total cloudiness in Figure 2 indicates that the incidence of overcast skies increases with cloud cover, so that where the cloud radiative forcing is large, the number of samples used to compute the clear sky flux is reduced. However, there are much fewer instances of missing data with this method compared with Method Ia.

Since the clear sky fluxes computed by Method Ib are dependent on sample size and are also weighted by the clear sky fraction, then they too may display a diurnal bias. As with Method Ia, this can be largely eliminated by the use of albedos in the calculation of the shortwave cloud forcing, with the result that the shortwave cloud forcings computed by Methods Ib and II are almost identical (Figure 10). The underestimation of the shortwave cloud forcing by Method Ia is mainly related to the areas of missing data where the large values of forcing are not sampled (Figures 5 and 7).

The difference in the longwave cloud forcings computed by the three methods (Figure 10) can be attributed to the tendency for Methods Ia and Ib to bias the clear sky flux towards that for drier and, over land, warmer conditions. The exception is near 10N where the underestimation of the forcing by Method Ia can again be related to the areas of missing data (Figures 6 and 8). The general overestimation of the longwave cloud forcing is not so marked with Method Ib because of the greater number of samples.

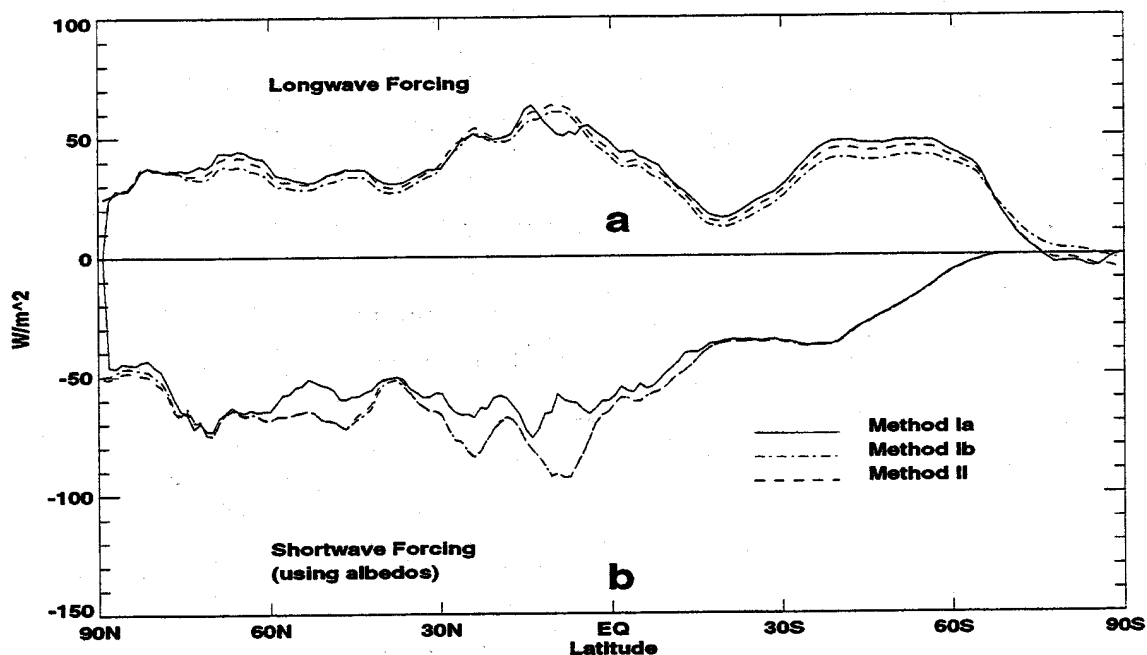


Fig. 10. The zonally averaged a) shortwave (using albedos) and b) longwave cloud forcings computed using Methods Ia, Ib and II, for the last 30 days of a T106 90-day perpetual July integration.

## 6. Discussion

### a. Intercomparison requirements

It is evident from the above results that the advantages of Method II are substantial when the purpose is model intercomparison or analysis of cloud feedback. Because Method II is free from any sampling biases, the clear sky fluxes can be compared readily between models, and the differences in the cloud radiative forcing can be directly related to differences in the physical parameterizations. On the other hand, Methods Ia and Ib are dependent on a host of characteristics specific to each

model which include the horizontal resolution, the type of cloud parameterization scheme employed (fractional or "on/off"), the presence of a diurnal cycle, and the length of the averaging period.

In addition, Methods Ia and Ib are only feasible if albedos rather than fluxes are used in the calculation of the shortwave cloud forcing. Strictly speaking this is incorrect since the cloud forcing should be thought of in terms of the energy loss or gain of the system due to clouds. For the shortwave, this is the effect of clouds on the absorption of solar radiation, and in the longwave, the effect of clouds on the thermal emission. The net cloud forcing (as with the net radiation) is the balance between the shortwave absorption and longwave emission and thus both components of the cloud forcing should be calculated in a consistent manner with the same temporal and spatial sampling.

*b. Sensitivities and cloud feedbacks.*

It is instructive to study how the various determinations of the clear sky fluxes influence the climate sensitivities in the framework of the surrogate climate change experiments of Cess et al. (1989,1990). Following the notation of that paper, a clear sky sensitivity  $\lambda_c$  and a total sensitivity are defined by the following expression:

$$\lambda, \lambda_c = \frac{1}{\frac{\Delta F}{\Delta T_s} - \frac{\Delta Q}{\Delta T_s}} \quad (7)$$

where  $\Delta F$  is the change in clear sky (total) outgoing longwave flux,  $\Delta Q$  the change in clear sky (total) absorbed solar radiation and  $\Delta T_s$  the change in global mean surface temperature. Table 1 lists the globally averaged values of all relevant fluxes in the control experiments and the differences in the same quantities between the SST+2K and SST-2K experiments. Clear sky fluxes and corresponding cloud radiative forcings are reported as obtained by Methods Ia, Ib and II, with albedos being used in the shortwave calculations for Methods Ia and Ib.

Table 1: Globally averaged values of relevant fluxes

	Control					
	T106	T21				
cloud amount (%)	53.11	55.95				
surface temperature (C)	16.57	17.18				
total OLR ( $Wm^{-2}$ )	245.98	240.80				
total absorbed SW ( $Wm^{-2}$ )	234.81	235.81				
	Method Ia		Method Ib		Method II	
clear-sky OLR ( $Wm^{-2}$ )	286.99	286.72	283.50	282.97	281.12	279.92
clear-sky abs SW ( $Wm^{-2}$ )	286.02	285.96	287.197	287.09	287.39	287.46
longwave forcing ( $Wm^{-2}$ )	38.41	43.84	37.52	42.15	35.14	39.11
shortwave forcing ( $Wm^{-2}$ )	-43.96	-38.75	-57.05	-50.09	-52.59	-51.65
net cloud forcing ( $Wm^{-2}$ )	-5.55	5.04	-19.53	-7.94	-17.45	-12.54
Changes (SST +2C) - (SST -2C)						
	T106	T21				
cloud amount (%)	-1.95	-1.76				
surface temperature (C)	3.40	3.47				
total OLR ( $Wm^{-2}$ )	5.66	7.63				
total abs SW ( $Wm^{-2}$ )	-4.87	-5.05				
$\lambda$ ( $Km^2W^{-1}$ )	0.32	0.27				
	Method Ia		Method Ib		Method II	
	T106	T21	T106	T21	T106	T21
clear-sky OLR ( $Wm^{-2}$ )	7.72	8.13	7.63	8.08	7.59	8.04
clear-sky abs SW ( $Wm^{-2}$ )	-0.27	-0.07	0.64	0.70	0.54	0.66
longwave forcing ( $Wm^{-2}$ )	1.49	0.29	1.97	0.44	1.94	0.41
shortwave forcing ( $Wm^{-2}$ )	-3.20	-2.88	-5.28	-5.79	-5.41	-5.71
net cloud forcing ( $Wm^{-2}$ )	-1.71	-2.58	-3.47	-5.31	-3.30	-5.35
$\lambda_c$ ( $Km^2W^{-1}$ )	0.44	0.42	0.45	0.47	0.48	0.47
$\lambda/\lambda_c=1+DCRF/G$	0.76	0.64	0.71	0.57	0.66	0.57

OLR, outgoing longwave radiation; SST, sea surface temperature

Although the results discussed in the previous sections were taken from an integration with the highest horizontal resolution, the analysis was also conducted for sets of integrations using lower resolution, more typical of those models the intercomparison study of Cess et al.(1989, 1990). Table 1 thus includes a summary of the results obtained with the T21 version of the model so that the dependence on resolution can also be addressed. This question is very relevant, since there is evidence that

some models may have a marked sensitivity to resolution in their distribution of humidity, and therefore cloudiness and corresponding fields (Kiehl and Williamson, 1991).

The global mean values for the control integrations confirm the earlier result that, independent of resolution, Method Ia overestimates the clear sky OLR because of its bias towards warmer and drier conditions. The clear sky shortwave absorption is underestimated by Method Ia, primarily because the areas of missing data are coincident with regions of large forcing, but also because these regions occur mainly over the tropical oceans (Figure 1) where the surface albedo is lower than for the extratropical oceans, bearing in mind the zenith angle dependence of albedo discussed in Section 3. Although Harshvardhan et al. (1989) attributed the large differences between Methods Ia and II clear sky shortwave absorptions in the UCLA/GLA GCM to the diurnal cycle in cloudiness, this effect has been largely eliminated in this study by use of albedos rather than fluxes for computing the shortwave cloud forcing.

The net cloud radiative forcing computed by Method Ia differs by more than  $10 \text{ Wm}^{-2}$  from that computed by Method II, the difference being greatest at lower resolution. Indeed, both the results from the control integrations and the changes associated with the SST perturbations show that the dependence on resolution is accentuated when Method Ia is used to compute the cloud radiative forcings and climate sensitivities. It should also be noted that the difference between Methods Ia and II exceeds the dependence on resolution identified in the Method II results.

The lower portion of Table 1 presents the changes and the climate sensitivity parameters calculated from the SST+2K and SST-2K integrations. As with all the GCMs reported in Cess et al. (1989, 1990), the total cloud amount decreases with an increase in SST. However, the magnitudes of both the shortwave and longwave cloud forcing increase. This can be attributed to the model's cloud radiative properties which are a function of cloud liquid water, the cloud liquid water content increasing with the warmer climate. The increase in cloud liquid water content influences the cloud's shortwave albedo more than its longwave emissivity so that the increase in shortwave forcing dominates, leading to a negative cloud feedback, characterized by a value of  $\lambda/\lambda_c$  which is less than unity.

Cess et al. (1989,1990) showed a large variation in sensitivities and cloud feedbacks obtained by various models with various resolutions, from weakly negative, as

in the ECMWF model, to strongly positive ( $\lambda\lambda_c$  in excess of 2). Some of this variation could be attributed to the differing resolutions, as identified in the comparison of the T21 and T106 results in Table 1.

It is evident from the comparison of Methods Ia, Ib and II given in Table 1 that uncertainties in the definition of the cloud radiative forcing itself do not greatly alter the climate sensitivity parameter for the ECMWF model. However, it is hoped that in the future much closer agreement between models on the sign and magnitude of the cloud feedback will be reached. In that case, the differences between the methods for computing cloud radiative forcing may be more critical. In this context, it should be noted from Table 1 that the difference in  $\Delta\text{CRF}$  between Methods Ia and II is comparable to the change in the net radiation associated with a doubling of  $\text{CO}_2$  (Schlesinger and Mitchell, 1987) and therefore must be considered important.

## 7. Conclusions

As shown in this study, only Method II allows the clouds radiative forcing to be defined clearly and simply without ambiguity, so that it can be readily compared from model to model. Method Ia, although discussed by Cess and Potter (1987) as being the closest in principle to the method used to derive cloud radiative forcing from satellite observations, suffers from a variety of problems. The results are highly dependent on the number and location of missing clear sky "observations" which generally occur in areas where the cloud radiative forcing is large. Moreover, different models will have different spatial and temporal distributions of these areas of missing clear sky "observations", which themselves depend on the length of the sampling period. If, as is suggested by those models that include interactive radiative properties, the cloud liquid water content feedback is a crucial process in climate change (e.g. Mitchell et al. 1989), then it is conceivable that it might go largely undetected with Method Ia, particularly if it occurs in regions already dominated by clouds.

As with Method Ia, the results from Method Ib are model-dependent through the cloud generation scheme, and are also affected by inadequate sampling of the diurnal cycle. The diurnal sampling bias can be substantial in the shortwave unless albedos are used instead of fluxes. Indeed, some of the differences between models found by Cess et al. (1989, 1990) may be attributed to the use of fluxes in the computation. Such

problems would be eliminated with Method II since a proper treatment of the diurnal cycle is assured with the clear sky fluxes defined at every time and every gridpoint.

As noted by Kiehl and Ramanathan (1990), Method I only produces cloud forcing diagnostics relevant to monthly mean time scales, and therefore cannot give any information on the diurnal cycle or the day-to-day variability in the cloud radiative forcing. Such information may be crucial to understanding the detailed interactions that link together the large-scale circulation, moist processes (in particular convection), clouds and radiation. In that respect, Method II would be more applicable since an intercomparison of climate models aimed at understanding the differences in sensitivities will have to address (among many other things) how these interactions are dealt with by the different models.

*Acknowledgments:* The authors would like to thank Professor Robert D. Cess for his valuable comments and inspiration and Dr. W. Lawrence Gates for his continuing support. We would also like to thank Robert Mobley, Robert Drach and Dean Williams for their programming efforts. The simulations were performed at the National Energy Research Supercomputer Center. This work was supported by the Environmental Sciences Division, Office of Energy Research, US Department of Energy and conducted at the Lawrence Livermore National Laboratory under US Department of Energy Contract W-7405-Eng-48 with the University of California.

## REFERENCES

- Alexander, R. C. and R. L. Mobley, 1978: Monthly average sea-surface temperature and icepack limits on a 1 global grid, *Mon. Wea. Rev.*, **104**, 143–148.
- Cess, R. D. and G. L. Potter, 1987: Exploratory studies of cloud radiative forcing with a general circulation model, *Tellus*, **39A**, 460–473.
- Cess, R. D., G. L. Potter, J.-P. Blanchet, G. L. Boer, S. J. Ghan, J. T. Kiehl, H. Le Treut, Z.X. Li, X. -Z. Liang, J. F. B. Mitchell, J. -J. Morcrette, D. A. Randall, M. R. Riches, E. Roeckner, U. Schlese, A. Slingo, K. E. Taylor, W. M. Washington, R. T. Wetherald and I. Yagai, 1969: Interpretation of cloud-climate feedback as produced by 14 atmospheric general circulation models. *Science*, **245**, 513–516.
- Cess, R. D., G. L. Potter, J.-P. Blanchet, G. L. Boer, A. D. Del Genio, M. Deque, V. Dymnikov, V. Galin, W. L. Gates, S. J. Ghan, J. T. Kiehl, A. A. Lacis, H. Le Treut, Z. X. Li, Z. -X. Liang, B. J. McAvaney, V. P. Meleshko, J. F. B. Mitchell, J. -J. Morcrette D. A. Randall, L. Rikus, E. Roeckner, J. -F. Royer, U. Schlese, D. A. Sheinin, A. Slingo, A. P. Sokolov, K. E. Taylor, W. M. Washington, R. T. Wetherald and I. Yagai, and M.-H. Zhang, 1990: Intercomparison and interpretation of climate feedback processes in 19 atmospheric general circulation models. *J. Geophys. Res.*, **95D**, 16,601–16,617.
- Cess, R. D., G. L. Potter, W. L. Gates, J.-J. Morcrette and L. Corsetti, 1992: Comparison of general circulation models to Earth Radiation Budget Experiment data: Computation of clear-sky fluxes, *J. Geophys. Res.*, **97**, 20,421–20,426.
- Coakley, J. A., Jr., and D. G. Baldwin, 1984: Towards the objective analysis of clouds from satellite imagery data, *J. Climate Appl. Meteor.*, **23**, 1065–1099.
- Harrison, E. F., D. R. Brooks, P. Minnis, B. A. Wielicki, W. F. Staylor, G. G. Gibson, D. F. Young, F. M. Denn and the ERBE Science Team, 1988: First estimates of the diurnal variation of longwave radiation from the multiple-satellite Earth Radiation Budget Experiment (ERBE), *Bull. Amer. Meteor. Soc.*, **69**, 1144–1151.

- Harshvardhan, D. A. Randall, T. G. Corsetti and D. A. Dazlich, 1988: Earth radiation budget and cloudiness simulations with a general circulation model. *J. Atmos. Sci.*, **46**, 1922–1942.
- Hollingsworth, A., A. Lorenc, M. S. Tracton, K. Arpe, G. Cats, S. Uppala and P. Kallberg, 1985: The response of numerical weather prediction systems to FGEE level II-b data. Part I: Analysis, *Quart. J. Roy. Meteor. Soc.*, **111**, 1–66.
- Kiehl, J. T. and V. Ramanathan, 1990: Comparison of cloud forcing derived from the Earth Radiation Budget Experiment with that simulated by the NCAR Community Climate Model, *J. Geophys. Res.*, **95**, 11,679–11,698.
- Kiehl, J. T. and D. L. Williamson, 1991: Dependence of cloud amount on horizontal resolution in the NCAR Community Climate, *J. Geophys. Res.*, **95**, 10,955.
- Minnis, P. and E. F. Harrison, 1984: Diurnal variability of regional cloud and clear-sky radiative parameters derived from GOES data. Part II: November 1978, cloud distributions, *J. Climate Appl. Meteor.*, **23**, 1012–1031.
- Mitchell, J. F. B., C. A. Senior and W. J. Ingram, 1989: CO<sub>2</sub> and climate: A missing feedback? *Nature*, **341**, 132–134.
- Morcrette, J.-J., 1990: Impact of changes to the radiative transfer parameterizations plus cloud optical properties in the ECMWF model, *Mon. Wea. Rev.*, **118**, 847–873.
- Ramanathan, V., 1987: The role of Earth Radiation Budget studies in climate and general circulation research, *J. Geophys. Res.*, **92**, 4075–4095.
- Schlesinger, M. E. and J. F. B. Mitchell, 1987: Model projections of the equilibrium climatic response to increased CO<sub>2</sub>, *Rev. Geophys.*, **89**, 760–798.

Simmons, A. J., D. M. Burridge, M. Jarraud, C. Girard and W. Wergen, 1988: The ECMWF medium-range prediction models, Development of the numerical formulations and the impact of increased resolution, *Meteor. Atmos. Phys.*, **40**, 28-60.

Slingo, J. M., 1987: The development and verification of a cloud prediction scheme for the ECMWF model, *Quart. J. Roy. Meteor. Soc.*, **113**, 899-928.

Tiedtke, M. A., 1989: comprehensive mass-flux scheme for cumulus parameterization in large-scale models, *Mon. Wea. Rev.*, **117**, 1779-1800.

Tiedtke, M., W. A. Heckley and J. M. Slingo, 1988: Tropical forecasts at ECMWF: On the influence of physical parameterization on the mean structure of forecasts and analyses, *Quart. J. Roy. Meteor. Soc.*, **114**, 639-664.